

Single polarization and poling optimized twin-hole optical fiber

Lin Huang (黄琳)^{1,2} and Guobin Ren (任国斌)^{1,2*}

¹Key Lab of All Optical Network & Advanced Telecommunication Network of EMC,
Beijing Jiaotong University, Beijing 100044, China

²Institute of Lightwave Technology, Beijing Jiaotong University, Beijing 100044, China

*Corresponding author: gbren@bjtu.edu.cn

Received May 24, 2014; accepted July 16, 2014; posted online January 16, 2015

We investigate optimal twin-hole poling optical fiber configurations, including distances between core and each electrode, and poling voltage based on the two-dimensional charge dynamics model. We propose a poled fiber with optimized $\chi^{(2)}$ as well as single-polarization property. Small distance between core and anode guarantees the poled fiber with large $\chi^{(2)}$ in fiber core and large polarization-dependent loss. A maximum $\chi^{(2)}$ in the core region either outside or inside nonlinear layer can be realized by appropriately selecting edge-to-edge distance between core and cathode. The maximum $\chi^{(2)}$ in the core region can be even larger by increasing the poling voltage.

OCIS codes: 060.4370, 060.2430, 060.240, 060.2280.
doi: 10.3788/COL201513.S10603.

Due to the macroscopic inversion symmetry structure, even-order nonlinear susceptibilities ($\chi^{(2n)}$) were forbidden in glass-based materials, limiting its application in active optical devices. Thermal poling can break the symmetry structure and introduce a relatively large $\chi^{(2)}$ in silica glasses^[1-3] and waveguides^[4-6] via subjecting high voltage across the sample at elevated temperature. The poling process is mainly determined by charges migration, fast sodium ions and following slow ionized hydrogen ions. After poling, a second-order nonlinear active layer, including depletion region and ions exchange region (in the order of 3–80 μm in the one-dimensional silica glasses), is formed underneath the anode surface, accompanied with a strong electric field (E_{DC}). $\chi^{(2)}$ is introduced via $\chi^{(2)} = 3E_{\text{DC}}\chi^{(3)}$, where $\chi^{(3)}$ is the intrinsic third-order nonlinear susceptibility.

It has been proved that the introduced electric field is proportional to sample thickness^[1] in one-dimensional silica glasses. In addition, the zero potential condition after poling gives rise to reversed electric field outside nonlinear layer^[7] which is in the same order of magnitude compared with electric field in nonlinear layer in fiber due to the small distances between electrodes^[5]. However, for thermal poling in optical fiber, especially in twin-hole optical fiber, to the best of our knowledge, investigations on distances between core and electrodes for optimal electric field profile in both directions have not been reported. Polarization properties of metal filled twin-hole poling fiber have been investigated and found that the fiber provides high polarization-dependent loss (PDL) and relatively low propagation loss with a short distance between core and electrodes under appropriate fiber configurations^[8]. Based on the knowledge, a single polarization and poling optimized twin-hole optical fiber is possible. A two-dimensional charge dynamics model is established for numerical investigation of thermal

poling process based on the previous one-dimensional two charge dynamics model^[1]. In this letter, we investigate the fiber configurations, including edge-to-edge distances between core and electrodes, and poling voltage for optimizing the electric field inside and outside nonlinear layer as well as maximizing the utilization of reversed electric field while providing a large PDL and relative low propagation loss.

Here the simulations are based on the finite element method. The diagram of twin-hole optical fiber along with parameters is shown in Fig. 1. Edge-to-edge distance between core and anode and cathode are defined as d_1 and d_2 , respectively. Assuming the twin hole is filled with Ag electrodes, refractive indices of the core and cladding are 1.45 and 1.4444 at wavelength of 1.55 μm for a single-mode operation.

The two-dimensional charge dynamics model is proposed according to the previous one-dimensional charge dynamics model^[1], which can be described as

$$\begin{cases} \frac{\partial C_i}{\partial t} + \nabla \cdot (-D_i \nabla C_i + z_i \mu_i F C_i \nabla \Phi) = 0, \\ \nabla^2 \Phi = -\frac{F}{\varepsilon} \sum_i z_i C_i, \end{cases} \quad (1)$$

where $C(x, y, t)$ is the concentration of charge carriers, i is the kind of charge carrier, $\Phi(x, y, t)$ is the electric potential distribution during poling process, D is the diffusion coefficient which can be defined as $D_i = k_{\text{B}} T \mu_i / e$, and z , μ , F , k_{B} , and ε are charge species (positive or negative), mobility, Faraday constant, Boltzmann constant, and the permittivity of samples, respectively. Parameters for the equation are taken from Ref. [1].

We first demonstrated a large PDL and relatively low propagation loss as functions of d_1 and d_2 in the

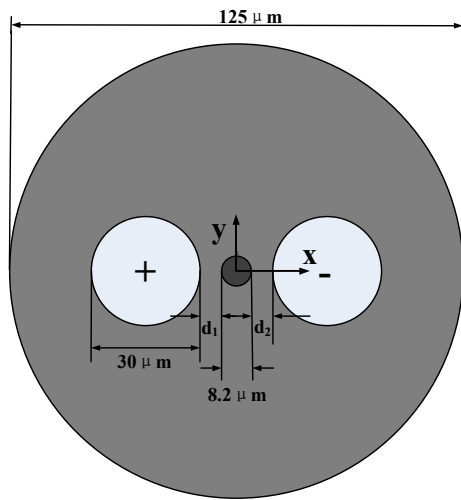


Fig. 1. Diagram of twin-hole optical fiber.

twin-hole fiber (Fig. 2). With a pair of Ag electrodes and radius of hole as $15 \mu\text{m}$, the results in Fig. 2 indicate that d_1 (or d_2) should be kept between 3 and $5 \mu\text{m}$ while d_2 (or d_1) should be kept larger than $3 \mu\text{m}$ if we want to obtain a high PDL as well as relatively low loss within the twin-hole poling/poled optical fiber with a length of dozens of centimeters. For $d_1 = d_2 = 3 \mu\text{m}$, the PDL is 598.23 dB/m and the propagation loss of y -polarization mode of HE_{11} mode is 35.22 dB/m, while $d_1 = d_2 = 5 \mu\text{m}$, the PDL and loss are 94.98 and 5.84 dB/m. By increasing d_2 from 3 to $9 \mu\text{m}$, the PDL spans from 598.23 to 261.23 dB/m, and propagation loss in the y -polarization mode spans from 35.22 to 16.70 dB/m. The loss can be further reduced from 16.70 to 7.75 dB/m by increasing the radius of the hole from 15 to $22 \mu\text{m}$, while the PDL barely changes.

For the purpose of realizing an optimum $\chi^{(2)}$ in the twin-hole fiber, we investigated the influence of distances between electrodes, including d_1 and d_2 on time evolution of average $\chi^{(2)}$ in core region based on the two-dimensional charge dynamics model. Results are shown in Figs. 3, 4 and 5.

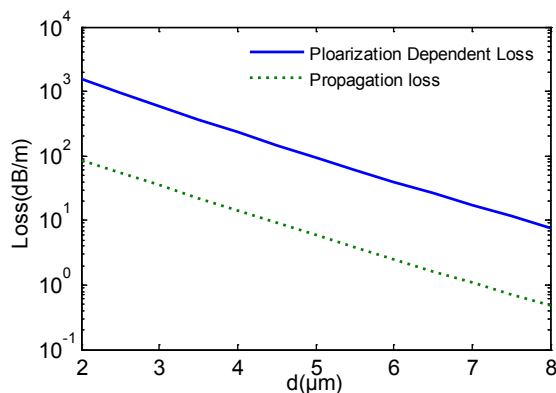


Fig. 2. (a) PDL and (b) propagation loss as functions of edge-to-edge distance between core and electrodes, d represents $d_1 = d_2$.

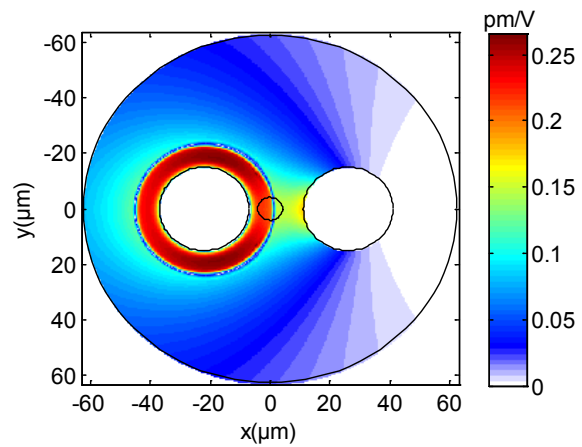


Fig. 3. Two-dimensional distributions of $\chi^{(2)}$ modulus after poling at $t = 3600 \text{ s}$, $d_1 = 3 \mu\text{m}$, and $d_2 = 7 \mu\text{m}$, poled at 5 kV, $250 \text{ }^\circ\text{C}$.

A typical two-dimensional $\chi^{(2)}$ distribution after poling is shown in Fig. 3. A nonlinear layer is located underneath anode surface with the electric field pointing from anode surface toward cathode and fiber outer surface. While outside the nonlinear layer, a reversed electric field is induced due to the zero potential condition. Time evolution of average $\chi^{(2)}$ in the core region with d_2 and d_1 varies as shown in Figs. 4 and 5.

In Fig. 4, with d_2 spanning from 3 to $9 \mu\text{m}$ while $d_1 = 3 \mu\text{m}$, time evolution of $\chi^{(2)}$ in core are quite the same with an abrupt increase followed by a decrease to zero and gradually increasing process. Note that the process is consistent with the Mach-Zehnder interferometer-based real-time electric-optic coefficient measurement in previous literature^[9,10], the after poling calculation leads to the discrepancy of model results and experimental results in previous literature which are measured in real-time during poling. Results in Fig. 4 indicate that two maximum average $\chi^{(2)}$ in opposite directions occur during poling, which depend on the poling time. For the purpose of optimizing, when d_1 is fixed, a smaller d_2 leads to a larger reversed $\chi^{(2)}$ in the core region for short poling

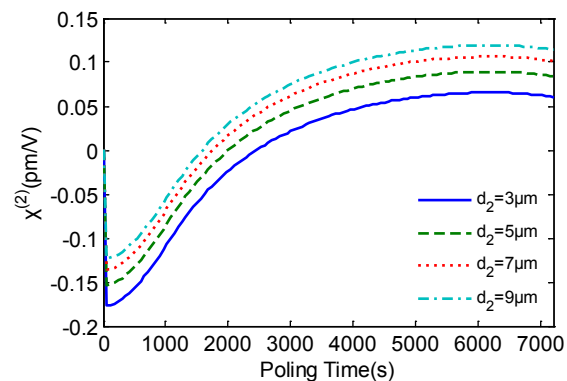


Fig. 4. Time evolution of average $\chi^{(2)}$ in fiber core after poling with d_2 varying, $d_1 = 3 \mu\text{m}$. Solid line, dashed line, dotted line, and dash-dot line represent $d_2 = 3, 5, 7,$ and $9 \mu\text{m}$, respectively.

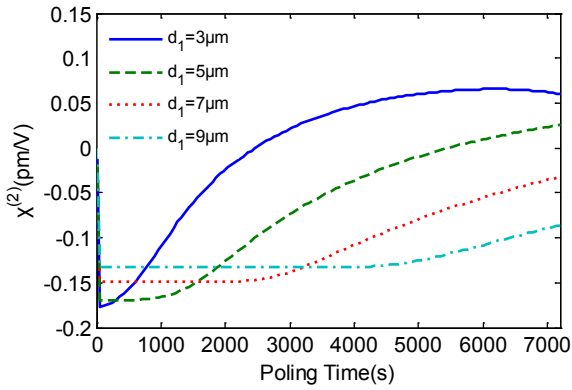


Fig. 5. Time evolution of average $\chi^{(2)}$ in fiber core after poling with d_1 varying, $d_2 = 3 \mu\text{m}$. Solid line, dashed line, dotted line, and dash-dot line represent $d_1 = 3, 5, 7,$ and $9 \mu\text{m}$, respectively.

time, whereas a larger d_2 leads to a larger positive $\chi^{(2)}$ for long poling time, that is, when $d_1 = d_2 = 3 \mu\text{m}$, the two maximum $\chi^{(2)}$ are -0.177 pm/V at 60 s (negative sign means a reversed direction compared with inside nonlinear layer) and 0.066 pm/V at 6180 s, respectively, when $d_1 = 3 \mu\text{m}$, $d_2 = 9 \mu\text{m}$, the $\chi^{(2)}$ are -0.123 pm/V at 60 s and 0.119 pm/V at 6180 s, respectively.

Results in Fig. 5 show that size of d_1 significantly affects the thermal poling results in the core region, which mainly determines the magnitude of introduced electric field and its coverage rate in the core region. It can be deduced that a smaller d_1 can lead to a larger average $\chi^{(2)}$ in the core region, either $\chi^{(2)}$ inside nonlinear layer or reversed $\chi^{(2)}$ outside nonlinear layer. The utilization of the two kinds of $\chi^{(2)}$ in opposite directions depends on poling time.

In addition to the fiber configurations, the poling voltage is another parameter for optimizing the $\chi^{(2)}$ in fiber core. Figure 6 shows the time evolution of average $\chi^{(2)}$ in fiber core after poling with different applied voltages. It is obvious that larger poling voltage contributes to larger maximum average $\chi^{(2)}$, with both the $\chi^{(2)}$ in opposite directions.

In conclusion, we investigate the optimal fiber configurations, including distances between core and anode and cathode, and poling voltage based on the two-dimensional charge dynamics model in association with the PDL and propagation loss in the metal/alloy filled twin-hole optical fiber. For the purpose of designing a single-polarization twin-hole optical fiber with optimal and effective $\chi^{(2)}$, it is necessary to decrease the edge-to-edge distance between core and anode. A maximum $\chi^{(2)}$ in the core region can be achieved with a small edge-to-edge

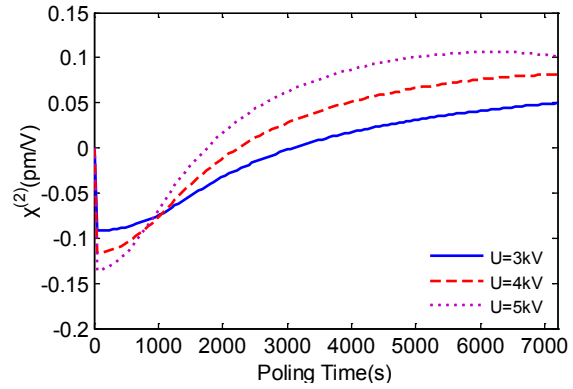


Fig. 6. Time evolution of average $\chi^{(2)}$ in fiber core after poling with applied voltage varying, $d_1 = 3, d_2 = 7 \mu\text{m}$. Solid line, dashed line, and dotted line represent $U = 3, 4,$ and 5 kV , respectively

distance between core and cathode for a short poling time (-0.177 pm/V) or a large edge-to-edge distance between core and cathode for a long poling time (0.119 pm/V). Meanwhile, a single-polarization twin-hole fiber can be achieved with the PDLs 598.23 and 261.23 dB/m, correspondingly. By increasing the poling voltage, the two maximum $\chi^{(2)}$ can be even larger. The poling optimized single-polarization twin-hole fiber is applicable for electro-optic modulators and switches.

This work was supported by the National Natural Science Foundation of China (No. 61178008) and the Fundamental Research Funds for the Central Universities, China.

References

1. A. Kudlinski, Y. Quiquempois, and G. Martinelli, *Opt. Express* **13**, 8015 (2005).
2. T. G. Alley, S. Brueck, and R. A. Myers, *J. Non-Cryst. Solids* **242**, 165 (1998).
3. R. A. Myers, N. Mukherjee, and S. R. Brueck, *Opt. Lett.* **16**, 1732 (1991).
4. H. An and S. Fleming, *Appl. Phys. Lett.* **89**, 231105 (2006).
5. N. Myrén and W. Margulis, *Opt. Express* **13**, 3438 (2005).
6. P. Blazkiewicz, W. Xu, D. Wong, and S. Fleming, *JOSA B* **19**, 870 (2002).
7. Y. Quiquempois, A. Kudlinski, and G. Martinelli, *JOSA B* **22**, 598 (2005).
8. L. Huang, G. Ren, B. Zhu, and X. Sun, *Opt. Commun.* **328**, 1 (2014).
9. W. Xu, J. Arentoft, D. Wong, and S. Fleming, *IEEE Photon. Technol. Lett.* **11**, 1265 (1999).
10. W. Xu, P. Blazkiewicz, D. Wong, S. Fleming, and T. Ryan, *Electron. Lett.* **36**, 1265 (2000).